Multi-element polynomial chaos with automatic discontinuity detection for nonlinear systems

Juliette Dréau[1*], Benoit Magnain[2] and Alain Batailly[1]

[1] Laboratoire d'Analyse Vibratoire et Acoustique, École Polytechnique de Montréal, Montréal, Canada
[2] LaMé, INSA CVL, Univ. Orléans, Univ. Tours, Bourges, France

31 July - 5 August 2022

POLYTECHNIQUE MONTRÉAL
UNIVERSITÉ D'INGÉNIERIE

INSA INSTITUT NATIONAL DES SCIENCES APPLIQUÉES CENTRE VAL DE LOIRE

WCCM-APCOM YOKOHAMA 2022
15th World Congress on Computational Mechanics & 8th Asian Pacific Congress on Computational Mechanics

Introduction
Context
Classical spectral methods
Methodology
Parameter analysis
Conclusion

Industrial context: turbomachine

Challenges

- maximizing performance
- reducing environmental footprint

Research investigations

$\Rightarrow$ improvement of the design of bladed disks to reduce at most the operating clearances

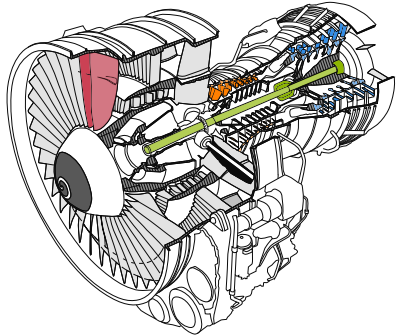

Industrial context: turbomachine

Challenges

- maximizing performance
- reducing environmental footprint

Research investigations

$\Rightarrow$ improvement of the design of bladed disks to reduce at most the operating clearances

Consequences

- favors nonlinear phenomena at certain interfaces
  - structural contacts at the blade-tip/casing interface

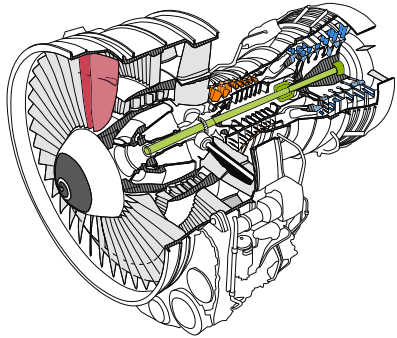

Study context

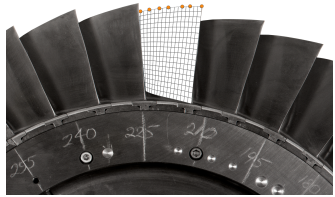

From *Colaïtis et al., 2021.*

Model from previous publications [1,2]

- a single blade of axial compressor NASA rotor 37 [3]
- equation of motion
  $\mathbf{M}\ddot{\mathbf{x}} + \mathbf{D}\dot{\mathbf{x}} + \mathbf{K}\mathbf{x} + \mathbf{f}_{nl}(\mathbf{x}, \dot{\mathbf{x}}) = \mathbf{f}_{ext}(\omega, t)$
- solved by explicit central finite difference time integration scheme and Lagrange multipliers for contact

Blade modeling

- 3D finite element model: 5745 nodes
- reduced-order model: Craig-Bampton model reduction [4] for a total of 34 dof
- modal damping
- blade clamped at its root and no centrifugal effects

Contact modeling

- rigid casing and no aerodynamic forcing $\mathbf{f}_{ext}(\omega, t) = 0$
- 8 boundary contact nodes ● along the blade-tip
- contact initiation: progressive distortion of the casing with 2 lobes

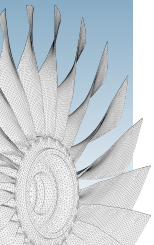

[1] E. Piollet et al. *J. Sound Vib.* (2019). doi: 10.1016/j.jsv.2019.114878. ISSN: 0022-460X
[2] Y. Colaïtis et al. *J. Eng. Gas Turbines Power* (2021). doi: 10.1115/1.4051967. ISSN: 0742-4795
[3] L. Reid et al. Technical report. NASA-TP-1337. NASA Lewis Research Center Cleveland, OH, United States, 1978
[4] R. R. Craig et al. *AIAA Journal* (1968). doi: 10.2514/3.4741

Study context

Quantity of Interest

- studied reponse: maximal radial displacement at the leading edge of the blade
- two parameters: angular frequency ω and operating clearance between the blade-tip and the casing c

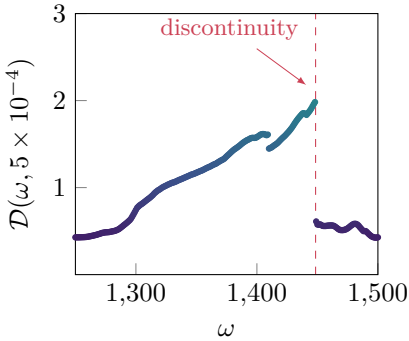

frequency response curve for a given clearance

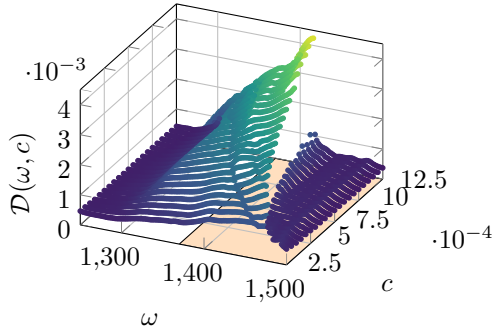

for several clearance values

Study context

Quantity of Interest

- studied reponse: maximal radial displacement at the leading edge of the blade
- two parameters: angular frequency ω and operating clearance between the blade-tip and the casing c

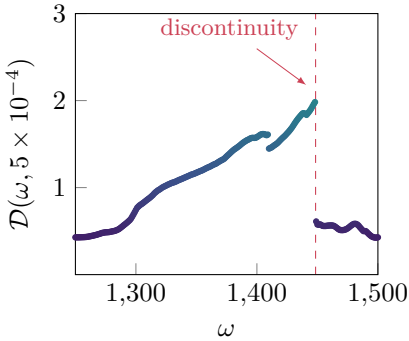

frequency response curve for a given clearance

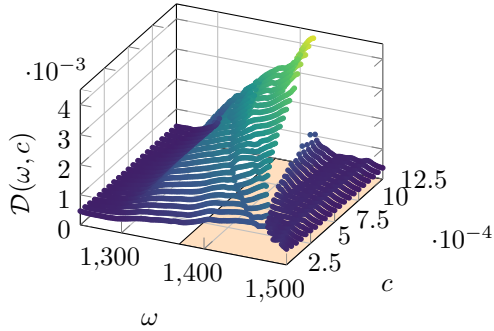

for several clearance values

Objective

approximate the response surface at lower cost by spectral method
major difficulty: discontinuity in the response surface

Surface approximation: classical methods

generalized Polynomial Chaos Expansion (gPCE) [5]

- expansion of the system response into a series of orthogonal polynomials
- continuous response $\Longrightarrow$ inaccurate results

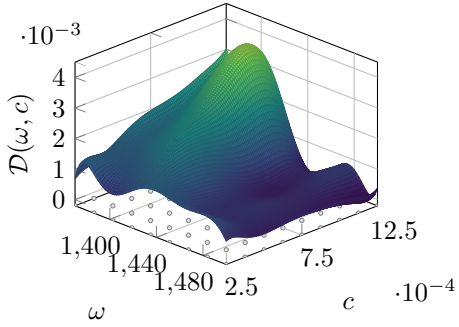

[5] D. Xiu et al. *SIAM J. Sci. Comput.* (2002). doi: 10.1137/S1064827501387826
[6] X. Wan et al. *J. Comput. Phys.* (2005). doi: 10.1016/j.jcp.2005.03.023. ISSN: 0021-9991

Introduction
Context
Classical spectral methods
Methodology
Parameter analysis
Conclusion

Surface approximation: classical methods

generalized Polynomial Chaos Expansion (gPCE) [5]

- expansion of the system response into a series of orthogonal polynomials
- continuous response $\Longrightarrow$ inaccurate results

Multi-Element generalized Polynomial Chaos Expansion (ME-gPCE) [6]

- piecewise gPCE: decomposition of the domain into several elements on which gPCE is applied
- tensor structure with rectangular shape elements $\Longrightarrow$ inaccurate results if the discontinuity is located in the element

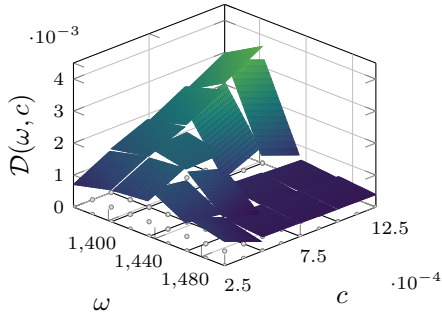

[5] D. Xiu et al. *SIAM J. Sci. Comput.* (2002). doi: 10.1137/S1064827501387826

[6] X. Wan et al. *J. Comput. Phys.* (2005). doi: 10.1016/j.jcp.2005.03.023. ISSN: 0021-9991

Surface approximation: classical methods

generalized Polynomial Chaos Expansion (gPCE) [5]

- expansion of the system response into a series of orthogonal polynomials
- continuous response $\Longrightarrow$ inaccurate results

Multi-Element generalized Polynomial Chaos Expansion (ME-gPCE) [6]

- piecewise gPCE: decomposition of the domain into several elements on which gPCE is applied
- tensor structure with rectangular shape elements $\Longrightarrow$ inaccurate results if the discontinuity is located in the element

Proposed methodology

domain decomposition according to the discontinuity of the studied response

[5] D. Xiu et al. *SIAM J. Sci. Comput.* (2002). doi: 10.1137/S1064827501387826
[6] X. Wan et al. *J. Comput. Phys.* (2005). doi: 10.1016/j.jcp.2005.03.023. ISSN: 0021-9991

Introduction
Methodology
Discontinuity detection
Domain decomposition
Response surface approximation
Parameter analysis
Conclusion

Contents

1 Introduction
Context
Classical spectral methods

2 Methodology
Discontinuity detection
Domain decomposition
Response surface approximation

3 Parameter analysis

4 Conclusion

Introduction
Methodology
Discontinuity detection
Domain decomposition
Response surface approximation
Parameter analysis
Conclusion

Proposed methodology

Steps

1. discontinuity detection
2. domain decomposition based on the detected discontinuities
3. gPCE approximation on each subdomain

Application to Rotor37

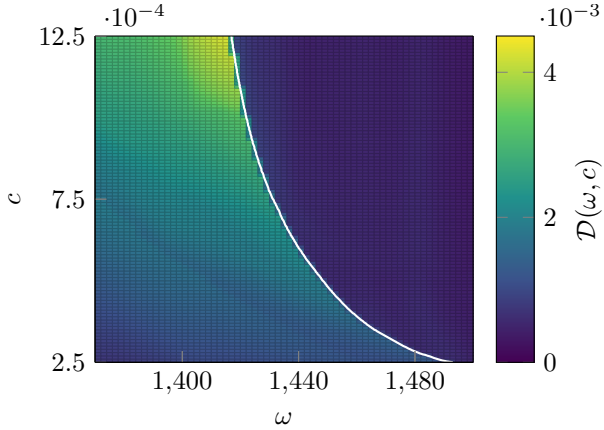

Discontinuity detection

Jump function

- defined in 1 dimension: $\delta f(x) = \lim_{\Delta \to 0} f(x + \Delta) - \lim_{\Delta \to 0} f(x - \Delta)$
- approximated by polynomial annihilation [7]

Initial mesh

- based on n_0-point regular grid (○) randomly shifted (●)
- computed a Delaunay triangulation (—): $\mathcal{T}^{(0)}$

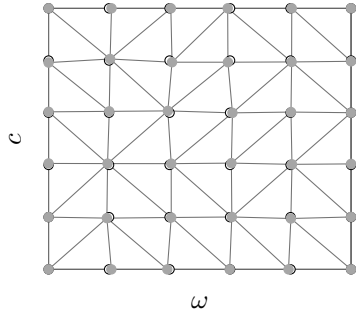

[7] R. Archibald et al. *SIAM J. Numer. Anal.* (2005). doi: 10.1137/S0036142903435259

Introduction
Methodology
Discontinuity detection
Edge detection
Localized refinement
Domain decomposition
Response surface approximation
Parameter analysis
Conclusion

Discontinuity detection

Iterative edge detection

1. approximate the jump values by polynomial annihilation on current mesh $\mathcal{T}^{(k)}$
2. identify the new point to add to the current mesh
   - identify the highest jump value triangle (□) and its two vertices (●)
   - compute the new point (●) as the middle of two vertices
   - verify a minimal distance
   - otherwise select the second highest jump value triangle

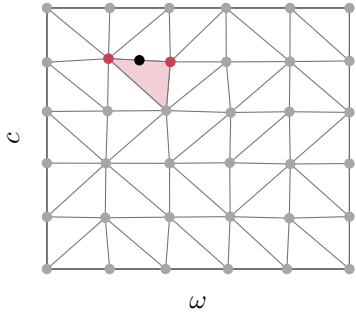

Introduction
Methodology
Discontinuity detection
Edge detection
Localized refinement
Domain decomposition
Response surface approximation
Parameter analysis
Conclusion

Discontinuity detection

Iterative edge detection

1. approximate the jump values by polynomial annihilation on current mesh $\mathcal{T}^{(k)}$
2. identify the new point to add to the current mesh
3. point labeling (-1 (●) or $+1$ (●)) and local remeshing of the Delaunay triangulation $\mathcal{T}^{(k+1)}$

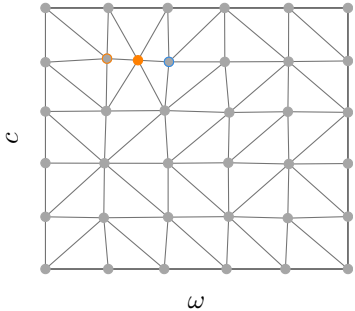

Introduction
Methodology
Discontinuity detection
Edge detection
Localized refinement
Domain decomposition
Response surface approximation
Parameter analysis
Conclusion

Discontinuity detection

Iterative edge detection

1. approximate the jump values by polynomial annihilation on current mesh $\mathcal{T}^{(k)}$
2. identify the new point to add to the current mesh
3. point labeling (-1 (●) or $+1$ (●)) and local remeshing of the Delaunay triangulation $\mathcal{T}^{(k+1)}$
4. repeat steps until one of the stopping criteria is satisfied:
   1. minimal jump value
   2. minimal distance between a new point and existing points
   3. maximal number of iteration

Discontinuity areas (□)

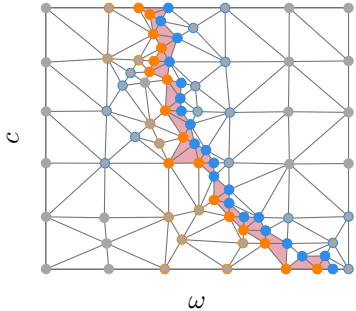

Introduction
Methodology
Discontinuity detection
Edge detection
Localized refinement
Domain decomposition
Response surface approximation
Parameter analysis
Conclusion

Discontinuity detection

Discontinuity description with Support Vector Machine

- apply support vector classification [8,9] from the training (●) (●) and test (○) (○) data
- obtain the decision boundary which is the discontinuity
- describe discontinuity by a B-spline [10]

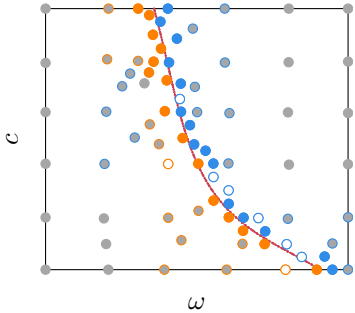

[8] C. M. Bishop et al. Springer, 2006

[9] J. Novakovic et al. *2011 IEEE 9th International Symposium on Intelligent Systems and Informatics*. doi: 10.1109/SISY.2011.6034373. 2011

[10] L. Piegl et al. doi: 10.1007/978-3-642-59223-2. Springer Berlin Heidelberg, 1997

Introduction
Methodology
Discontinuity detection
Edge detection
Localized refinement
Domain decomposition
Response surface approximation
Parameter analysis
Conclusion

Discontinuity detection

Localized refinement

1. identify the maximal distance between the nearest discontinuity points (●) (●) and spline (●–)
2. compute the new candidate point (▲) in the middle of the maximal distance: $\mathbf{x}_{k+1}$
3. verify that $\mathbf{x}_{k+1}$ is not too close to other points (□)
4. otherwise, change the new point by one in orthogonal direction (△): $\mathbf{x}^+$ or $\mathbf{x}^-$
5. update the spline

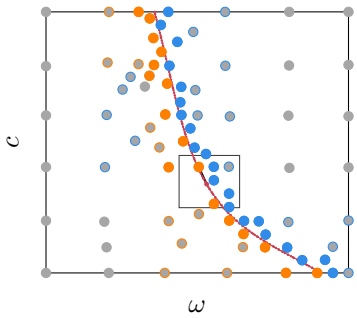

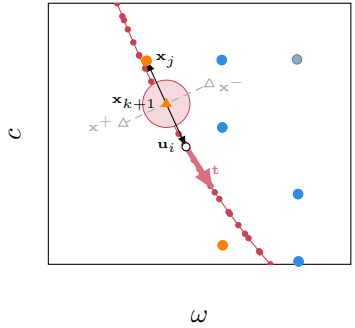

Zoom

Introduction
Methodology
Discontinuity detection
Edge detection
Localized refinement
Domain decomposition
Response surface approximation
Parameter analysis
Conclusion

Discontinuity detection

Localized refinement

1. identify the maximal distance between the nearest discontinuity points (●) (●) and spline (●-●-)
2. compute the new candidate point (▲) in the middle of the maximal distance: $\mathbf{x}_{k+1}$
3. verify that $\mathbf{x}_{k+1}$ is not too close to other points (□)
4. otherwise, change the new point by one in orthogonal direction (△): $\mathbf{x}^+$ or $\mathbf{x}^-$
5. update the spline

↻ repeat steps until the two stopping criteria are satisfied:

1. minimal distance between the nearest discontinuity points and the spline knots, based on previous publication [11]
2. minimal score of the SVM classification

[11] A. Gorodetsky et al. *SIAM J. Sci. Comput.* (2014). doi: 10.1137/140953137

Discontinuity detection

Application to Rotor37

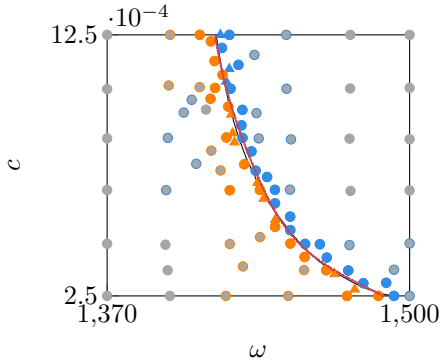

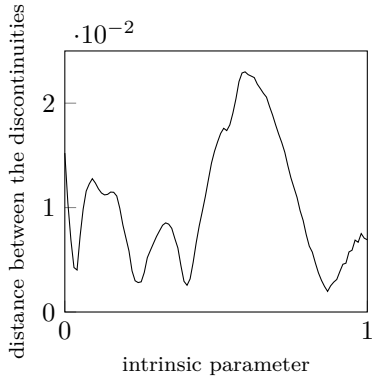

initial mesh (●)	edge detection (●) (●) (●) (●)	localized refinement (▲)(▲)	total
36	47	11	94

Introduction
Methodology
Discontinuity detection
Domain decomposition
Response surface approximation
Parameter analysis
Conclusion

Domain decomposition

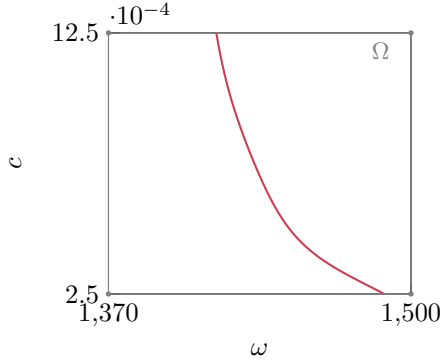

N non-overlapping subdomains such as:

$$\begin{cases} \Omega = \bigcup_{i=1}^{N} \Omega_i, \\ \forall i, j \in [\![1, N]\!], i \neq j \Leftrightarrow \Omega_i \cap \Omega_j = \emptyset. \end{cases} \tag{1}$$

Introduction
Methodology
Discontinuity detection
Domain decomposition
Response surface approximation
Parameter analysis
Conclusion

Domain decomposition

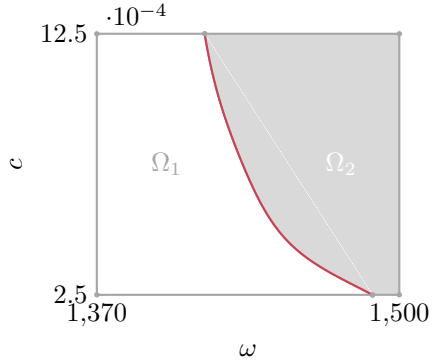

N non-overlapping subdomains such as:

$$\begin{cases} \Omega = \bigcup_{i=1}^{N} \Omega_i, \\ \forall i, j \in [\![1, N]\!], i \neq j \Leftrightarrow \Omega_i \cap \Omega_j = \emptyset. \end{cases} \quad (1)$$

Introduction
Methodology
Discontinuity detection
Domain decomposition
Response surface approximation
Parameter analysis
Conclusion

Domain decomposition

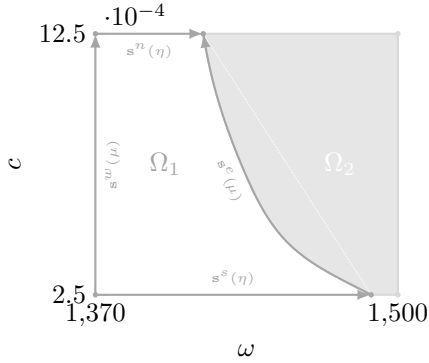

N non-overlapping subdomains such as:

$$\begin{cases} \Omega = \bigcup_{i=1}^{N} \Omega_i, \\ \forall i, j \in [\![1, N]\!], i \neq j \Leftrightarrow \Omega_i \cap \Omega_j = \emptyset. \end{cases} \tag{1}$$

Introduction
Methodology
Discontinuity detection
Domain decomposition
Response surface approximation
Parameter analysis
Conclusion

Response surface approximation

gPCE on each subdomain Ω_i with rectangular shape subdomain [12]

1. transformation into a reduced centered variable $\boldsymbol{\xi}$ as [13]:

$$T\colon [-1,1]^2 \to \Omega_i, \qquad \boldsymbol{\xi} \mapsto \mathbf{x} = T(\boldsymbol{\xi}), \quad \text{where } \mathbf{x} = [\omega, c] \tag{2}$$

   - linear transformation

2. response surface approximation defined as:

$$D(\boldsymbol{\xi}) \approx \sum_{j=0}^{p} \beta_j \Psi_j(\boldsymbol{\xi}), \tag{3}$$

3. construction of the polynomial basis Ψ_j
   - polynomials of degree lower or equal to q
   - Legendre polynomials
4. computation of the coefficients β_j
   - regression method [14]
   - system evaluations on a Design of Experiments (DoE)

[12] X. Wan et al. *J. Comput. Phys.* (2005). doi: 10.1016/j.jcp.2005.03.023. ISSN: 0021-9991

[13] D. Xiu et al. *SIAM J. Sci. Comput.* (2002). doi: 10.1137/S1064827501387826

[14] M. Berveiller et al. *Eur. J. Comp. Mech.* (2006). doi: 10.3166/remn.15.81-92

Introduction
Methodology
Discontinuity detection
Domain decomposition
Response surface approximation
Parameter analysis
Conclusion

Response surface approximation

gPCE on each subdomain Ω_i with proposed methodology

1. transformation into a reduced centered variable $\boldsymbol{\xi}$ as [13]:

$$T\colon [-1,1]^2 \to \Omega_i, \qquad \boldsymbol{\xi} \mapsto \mathbf{x} = T(\boldsymbol{\xi}), \quad \text{where } \mathbf{x} = [\omega, c] \tag{2}$$

   - transfinite transformation [15] defined by the subdomain boundaries

2. response surface approximation defined as:

$$D(\boldsymbol{\xi}) \approx \sum_{j=0}^{p} \beta_j \Psi_j(\boldsymbol{\xi}), \tag{3}$$

3. construction of the polynomial basis Ψ_j
   - polynomials of degree lower or equal to q
   - Legendre polynomials
4. computation of the coefficients β_j
   - regression method [14]
   - system evaluations on a Design of Experiments (DoE)

[13] D. Xiu et al. *SIAM J. Sci. Comput.* (2002). doi: 10.1137/S1064827501387826
[15] W. J. Gordon et al. *Numer. Math.* (1973). doi: 10.1007/BF01436298
[14] M. Berveiller et al. *Eur. J. Comp. Mech.* (2006). doi: 10.3166/remn.15.81-92

Introduction
Methodology
Discontinuity detection
Domain decomposition
Response surface approximation
Parameter analysis
Conclusion

Response surface approximation

Transfinite transformation on Ω_i

- smooth mapping from a boundary to another
- example from a points grid:

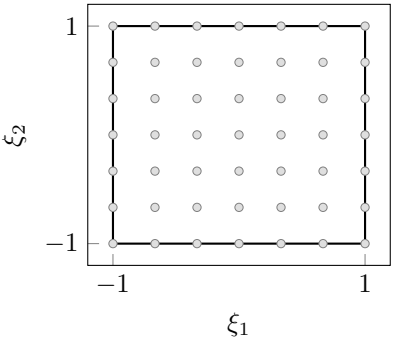

(a) grid of $\boldsymbol{\xi}$

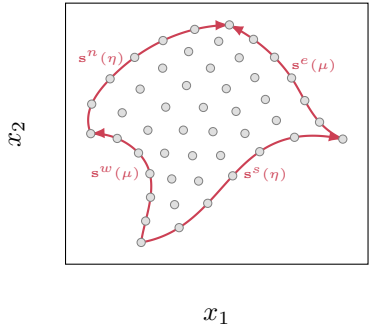

(b) transfinite transformation of $\boldsymbol{\xi}$ for subdomain boundaries (▬)

Response surface approximation

Design of Experiments

- points from discontinuity detection step
- inverse transformation T^{-1} for each point ( )
  - solve by Newton-Raphson procedure [16]
  - reduce numerical cost by a minimum spanning tree [17] ( ) and a nearest neighbor search [18]
  - starting point ( ) at the center of the domain

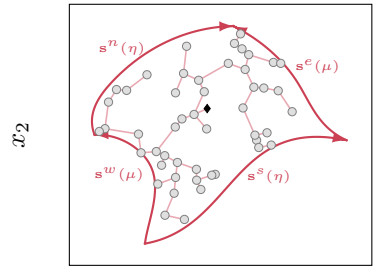

(a) DoE points and subdomain boundaries ( )

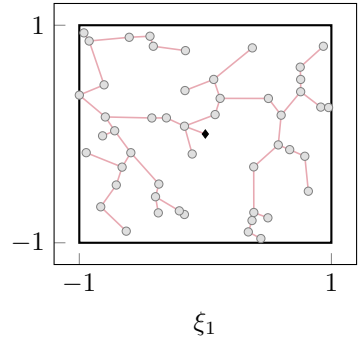

(b) inverse transfinite transformation of DoE points

[16] R. Burden et al. Cengage Learning, 2010. ISBN: 9781133169338

[17] M. Held et al. *Operations Research* (1970). doi : 10.1287/opre.18.6.1138. ISSN: 0030364X, 15265463

[18] M. Bellmore et al. *Oper. Res.* (1968)

Introduction
Methodology
Discontinuity detection
Domain decomposition
Response surface approximation
Parameter analysis
Conclusion

Response surface approximation

Application to Rotor37

- design of experiments: 94 points in Ω
  - separate the points between the two subdomains: 51 points (○) in Ω_1 and 43 points (●) in Ω_2
  - verify that the points are on the right side of the discontinuity thanks to their labels

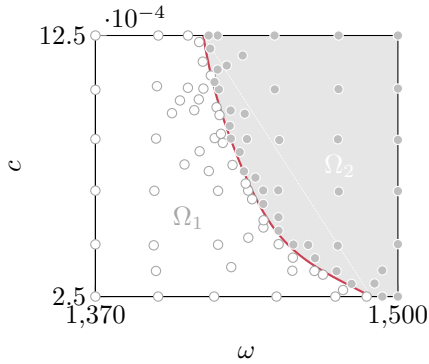

Response surface approximation

Application to Rotor37

- design of experiments: 94 points in Ω
  - separate the points between the two subdomains: 51 points (○) in Ω_1 and 43 points (●) in Ω_2
  - verify that the points are on the right side of the discontinuity thanks to their labels
- results with degree $q = 4$ $\Longrightarrow$ accurate results

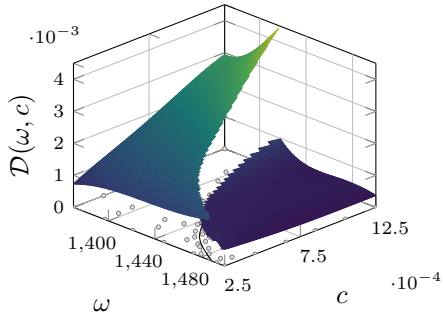

(a) approximated response surface with the proposed methodology

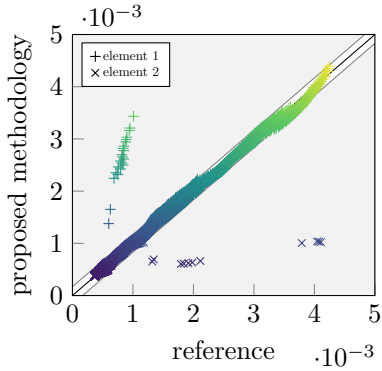

(b) scatter plot

Contents

1 Introduction
Context
Classical spectral methods

2 Methodology
Discontinuity detection
Domain decomposition
Response surface approximation

3 Parameter analysis

4 Conclusion

Parameter analysis

Variation of two parameters

1. stopping criterion on the minimal jump value of the edge detection
   - decrease minimal jump value $\Longrightarrow$ increase edge detection iteration and computational cost
   - increase minimal jump value $\Longrightarrow$ increase localized refinement iteration and obtain an aberrant shaped discontinuity

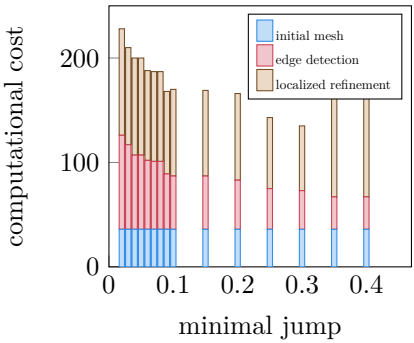

(a) computational cost

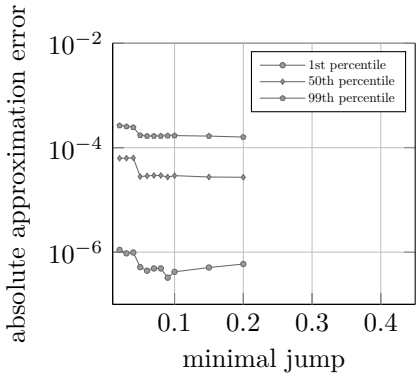

(b) percentiles of absolute approximation error

Parameter analysis

Variation of two parameters

1. stopping criterion on the minimal jump value of the edge detection
   - decrease minimal jump value $\Longrightarrow$ increase edge detection iteration and computational cost
   - increase minimal jump value $\Longrightarrow$ increase localized refinement iteration and obtain an aberrant shaped discontinuity
2. stopping criterion on the minimal distance of the localized refinement
   - decrease minimal distance $\Longrightarrow$ increase refinement iteration and computational cost
   - similar approximation errors

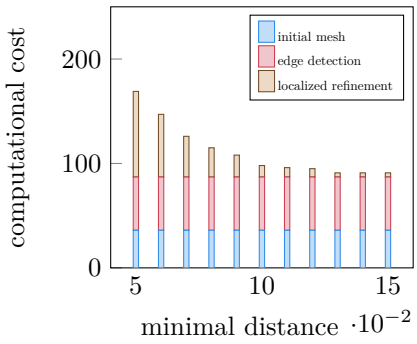

(a) computational cost

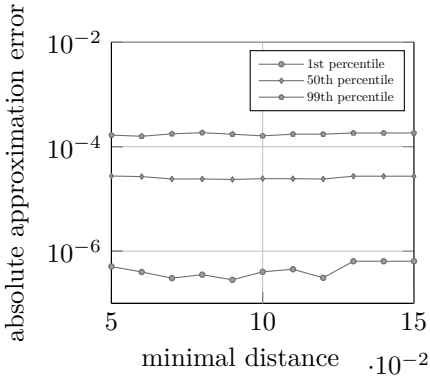

(b) percentiles of absolute approximation error

Contents

1 Introduction
Context
Classical spectral methods

2 Methodology
Discontinuity detection
Domain decomposition
Response surface approximation

3 Parameter analysis

4 Conclusion

Conclusion

Proposed methodology

- automated detection of discontinuities relying on a two-step approach:
  1. iterative edge detection
  2. localized refinement to accurately represent the discontinuities by means of B-spline curves
- approximation of the response surface using a domain decomposition for an optimal application of ME-gPCE

Application of the proposed methodology

- complex system of the Rotor37 blade with accurate results
- other academic systems with accurate results

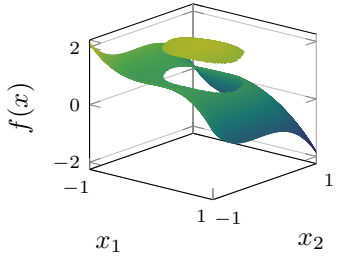

(a) circular discontinuity used in the literature [19]

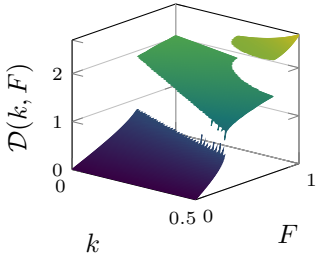

(b) Duffing oscillator with added discontinuity

[19] J. D. Jakeman et al. *J. Comput. Phys.* (2013). doi: 10.1016/j.jcp.2013.02.035. ISSN: 0021-9991

Thank you for your attention